

## Competing effects of surface phonon softening and quantum size effects on the superconducting properties of nanostructured Pb

This article has been downloaded from IOPscience. Please scroll down to see the full text article.

2009 J. Phys.: Condens. Matter 21 205702

(<http://iopscience.iop.org/0953-8984/21/20/205702>)

View [the table of contents for this issue](#), or go to the [journal homepage](#) for more

Download details:

IP Address: 129.252.86.83

The article was downloaded on 29/05/2010 at 19:44

Please note that [terms and conditions apply](#).

# Competing effects of surface phonon softening and quantum size effects on the superconducting properties of nanostructured Pb

Sangita Bose<sup>1,3</sup>, Charudatta Galande<sup>1</sup>, S P Chockalingam<sup>1</sup>,  
Rajarshi Banerjee<sup>2</sup>, Pratap Raychaudhuri<sup>1</sup> and Pushan Ayyub<sup>1</sup>

<sup>1</sup> Department of Condensed Matter Physics and Material Science, Tata Institute of Fundamental Research, Mumbai 400005, India

<sup>2</sup> Department of Materials Science and Engineering, University of North Texas, Denton, TX 76203-5310, USA

E-mail: [Sangita.Bose@fkf.mpg.de](mailto:Sangita.Bose@fkf.mpg.de), [pratap@tifr.res.in](mailto:pratap@tifr.res.in) and [pushan@tifr.res.in](mailto:pushan@tifr.res.in)

Received 16 December 2008, in final form 20 March 2009

Published 24 April 2009

Online at [stacks.iop.org/JPhysCM/21/205702](http://stacks.iop.org/JPhysCM/21/205702)

## Abstract

The superconducting transition temperature ( $T_C$ ) in nanostructured Pb decreases from 7.24 to 6.4 K as the particle size is reduced from 65 to 7 nm, below which superconductivity is lost rather abruptly. In contrast, there is a large enhancement in the upper critical field ( $H_{C2}$ ) in the same size regime. We explore the origin of the unusual robustness of  $T_C$  over such a large particle size range in nanostructured Pb by measuring the temperature dependence of the superconducting energy gap in planar tunnel junctions of Al/Al<sub>2</sub>O<sub>3</sub>/nano-Pb. We show that below 22 nm, the electron–phonon coupling strength increases monotonically with decreasing particle size, and almost exactly compensates for the quantum size effect, which is expected to suppress  $T_C$ .

(Some figures in this article are in colour only in the electronic version)

Superconductivity at reduced length scales has been a subject of intense research over the past few decades [1–11]. Though one may expect changes in the superconducting properties as the system size is reduced below the fundamental length scales such as the coherence length,  $\xi(T)$ , and the penetration depth,  $\lambda_L(T)$ , it is now established that there is actually a *third* length scale that finally defines a zero-dimensional superconductor. This is the critical particle diameter ( $D_C$ ) at which the energy level spacing (the ‘Kubo’ gap,  $\delta$ ) arising from the discretization of the energy bands equals the superconducting energy gap ( $\Delta(0)$ ). Superconductivity is completely destabilized below this length scale; this is the ‘Anderson criterion’ [2] for the destruction of superconductivity. The existence of the ‘Anderson criterion’ has been successfully demonstrated in many elemental superconductors such as Al [3], Sn [5], In [12], Pb [6, 7] and Nb [13]. However, as the size

of the superconductor approaches  $D_C$ , the behavior of the superconducting transition temperature ( $T_C$ ) is quite different in different systems: superconductors with a weak electron–phonon coupling (In, Al and Sn) show an increase in  $T_C$ ; the intermediate coupling superconductor Nb shows a gradual, monotonic decrease in  $T_C$ ; while the  $T_C$  in the strong coupling superconductor, Pb, shows almost no change.

The evolution of  $T_C$  in nanostructured superconductors is normally understood in terms of the competition between two effects. The first arises from the increase in surface to volume ratio with decreasing size. As the surface atoms have a smaller coordination number than the bulk atoms, surface phonons are softer than bulk phonons. This leads to an overall decrease in the phonon frequencies in nanoparticles [14], resulting in an enhanced electron–phonon coupling strength [15] and a higher  $T_C$ . Experimentally, an increase in the electron–phonon coupling can be detected by measuring the dimensionless quantity  $2\Delta(0)/k_B T_C$ , which monotonically increases with

<sup>3</sup> Present address: Max Planck Institute for Solid state Research, Nanoscale Science Department, Stuttgart, Germany.

coupling strength from its value of 3.52 in the weak coupling limit. This effect could be counteracted by the quantum size effect (QSE) arising from the discretization of the electronic energy bands in small particles and leading to a decrease in the effective density of states,  $N(0)$ , at the Fermi level [16, 17]. A decrease in  $N(0)$  for a strong coupling superconductor would lead to a decrease in  $2\Delta(0)/k_B T_C$  with a reduction in the particle size. To distinguish between the effects of these two mechanisms in nanostructured superconductors, it is necessary to make independent measurements of  $T_C$  and  $\Delta(0)$  as a function of particle size.

We have previously shown [13] that in nanocrystalline thin films of Nb, QSEs become apparent below  $\approx 20$  nm. The QSE-induced reduction in the density of states at the Fermi level decreases  $T_C$  to almost 50% of its bulk value as the particle size is reduced from 20 to 8 nm. In the strong coupling superconductor Pb, the bulk superconducting energy gap ( $\Delta(0) \approx 1.38$  meV) as well as the critical size at which superconductivity gets destroyed ( $D_C \approx 6$  nm) are close to the corresponding values in Nb. One may therefore expect QSEs to play similar roles in Pb and Nb. The size dependence of  $T_C$  in Pb is, however, qualitatively different from that in Nb, decreasing by only  $\approx 13\%$  as the particle size is reduced [6, 7] from bulk to 7 nm, below which it becomes non-superconducting. To understand the robustness of  $T_C$  with decreasing size in Pb, we carried out simultaneous measurements of  $\Delta(0)$  and  $T_C$  in planar tunnel junctions consisting of Al,  $\text{Al}_2\text{O}_3$  and nanostructured Pb films (with different values of the average grain diameter,  $D$ ), grown by high-pressure magnetron sputter deposition. Interestingly,  $\Delta(0)$  was found to increase with decreasing size (for  $D < 20$  nm) though  $T_C$  remained virtually constant. A measurement of the temperature variation of the gap further indicates a size-dependent deviation from the weak coupling BCS behavior in nanostructured Pb, implying an enhancement of the electron-phonon coupling strength. Our results suggest that in nano-Pb, the expected decrease in  $T_C$  due to the QSE is almost exactly offset by the increase in electron-phonon coupling strength, down to the Anderson limit.

Nanocrystalline films of Pb ( $\approx 200$  nm thick) were deposited on glass substrates by high-pressure magnetron sputtering from elemental Pb targets (Kurt and Lesker, 99.999%). The particle size was varied in the range 5–60 nm by controlling the sputtering gas (Ar) pressure, the applied power and the deposition time. To prevent oxidation, the nanocrystalline Pb films were capped with a 40 nm thick overlayer of Si grown *in situ* using RF-sputtering. The mean particle size ( $D$ ) and size distribution were determined from x-ray diffraction (XRD) line profile analysis, using WINFIT software, and transmission electron microscopy (TEM). The particle sizes measured by the two methods matched closely. The particle size distribution in each film was approximately  $\pm 15\%$ . Figures 1(a) and (b) show the bright field TEM patterns obtained from samples with  $D_{\text{XRD}} = 60$  and 14 nm, respectively; the insets showing the corresponding selected area diffraction patterns. The high resolution TEM image of the  $D_{\text{XRD}} = 5$  nm sample (figure 1(c)) shows crystalline Pb grains of

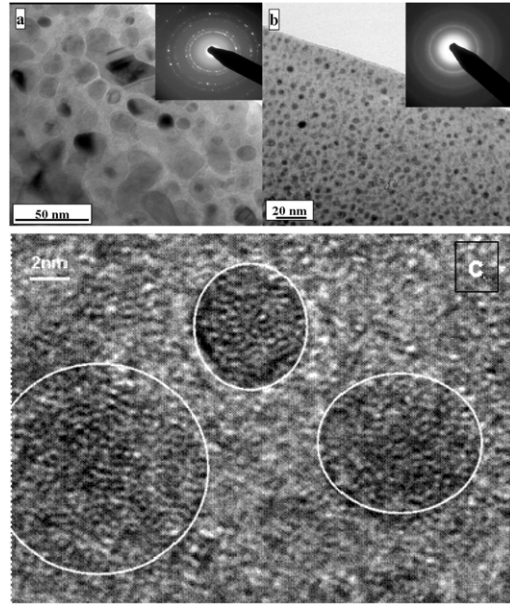


**Figure 1.** Bright field TEM images of the nanostructured Pb films with particle size (a)  $D_{\text{XRD}} = 60$  nm and (b)  $D_{\text{XRD}} = 14$  nm, the corresponding selected area diffraction patterns being shown in the insets. (c) High resolution TEM image of the film with  $D_{\text{XRD}} = 5$  nm showing Pb grains (marked by circles) separated by a disordered intergranular region.

$\approx 5$  nm diameter (darker contrast) separated by a disordered intergranular region, possibly consisting of an amorphous Pb–O phase<sup>4</sup>. Magnetic and transport measurements were carried out down to 2.2 K using a home-made planar coil ac susceptometer and a magneto-transport setup, respectively. In the planar coil setup, the superconducting film is sandwiched between two 100-turn miniature coils and the susceptibility is determined by measuring the mutual inductance between the two coils. Details of this measurement technique can be found elsewhere [21]. The resistance was measured using the conventional four-probe technique after evaporating four silver pads on the film. The superconducting energy gap ( $\Delta$ ) was measured by fabricating planar tunnel junctions of Al/ $\text{Al}_2\text{O}_3$ /nano-Pb films by a standard method [19]. 1 mm Al strips were thermally evaporated through a mask on a glass side (thoroughly cleaned in boiling acetone and vapor cleaned in trichlorethylene and propanol). The Al film was oxidized by exposure to air for 20 min. Nanostructured Pb films were then sputter deposited as cross strips on the  $\text{Al}_2\text{O}_3$  layer using proper masks to produce, on each device, two Al/ $\text{Al}_2\text{O}_3$ /nano-Pb tunnel junctions with effective junction areas of  $1 \times 1$  mm<sup>2</sup>. For the tunnel junction with the largest particle size ( $D_{\text{XRD}} = 64$  nm) the Pb strip was thermally evaporated at high vacuum.

Figures 2(a) and (b) show the temperature dependence of the ac magnetic susceptibility and the dc resistance<sup>5</sup>

<sup>4</sup> Similar structure was also observed in nanocrystalline Nb films where electron energy loss spectroscopy confirmed the granular and intergranular region to be Nb and  $\text{Nb}_2\text{O}_5$ , respectively; see [18].

<sup>5</sup> We could not determine the resistivity of the films due to the Si protective layer that needed to be deposited to prevent oxidation.

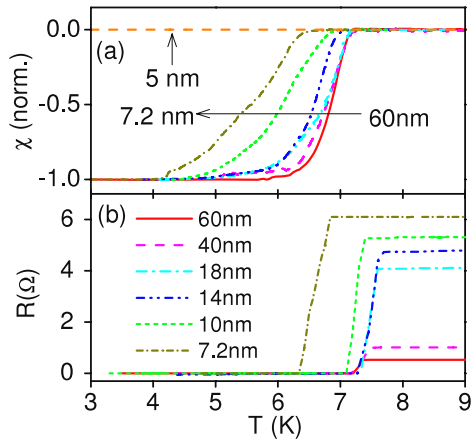
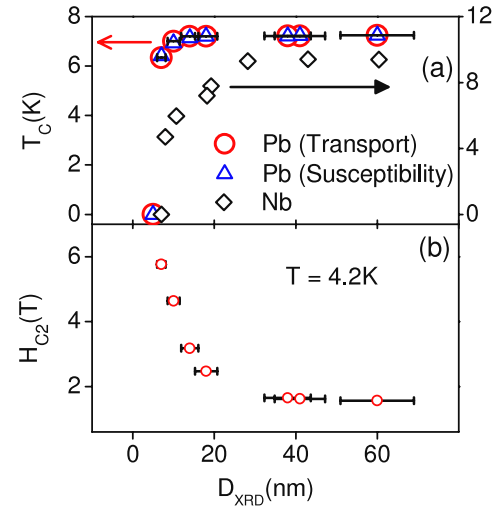


**Figure 2.** Temperature dependence of (a) the normalized ac susceptibility and (b) the dc electrical resistance of the nanostructured Pb films with different particle sizes.

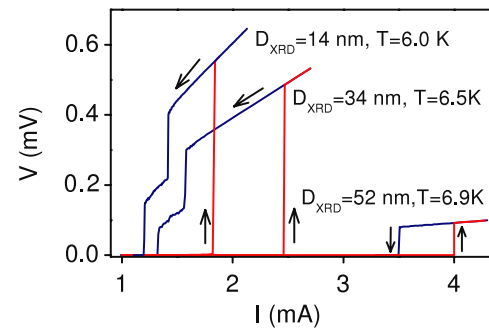
for the nano-Pb films with different particle size. Using commonly accepted criteria,  $T_C$  was estimated (i) from transport measurements as the temperature at which the resistance dropped to 10% of its normal state value, and (ii) from ac susceptibility measurements as the temperature at which the real part of the susceptibility deviated from zero. The  $T_C$  obtained from the two methods matched almost exactly (figure 3(a)). We observe that  $T_C$  does not deviate from the bulk value (7.24 K) down to  $D \approx 14$  nm and decreases by only  $\approx 13\%$  between 14 and 7 nm (figure 3(a)). Below 7 nm, Pb loses its superconductivity quite abruptly. We can estimate the critical size below which superconductivity is destroyed using the Anderson criterion [2] from an estimation of the Kubo gap:  $\delta = 4E_F/3N$ , where  $E_F$  is the Fermi energy and  $N$  is the number of electrons in a grain. Using [20]  $E_F = 9.37$  eV and the electron density  $n = 13.2 \times 10^{22}$  electrons  $\text{cm}^{-3}$  we obtain this critical size as 7 nm, which agrees closely with our observation. Our result is in qualitative agreement with the size variation of  $T_C$  in Pb reported by other groups [6, 7]. Importantly, figure 3(a) also brings out the qualitative difference in the size dependence of  $T_C$  in nano-Pb and nano-Nb (data from [13]). In the intermediate coupling superconductor Nb, a *gradual* depression of  $T_C$  starts at comparatively large sizes (above 20 nm) and the  $T_C$  decreases by about 50% down to 8 nm, below which it becomes non-superconducting.

Figure 3(b) shows the size dependence of the upper critical field ( $H \parallel$  film plane) of nanostructured Nb, measured at 4.2 K. The  $H_{C2}(T = 4.2 \text{ K})$ , shows a monotonic increase with decreasing size down to 7 nm, consistent with previous results [7]. In nano-Nb,  $H_{C2}$  shows a non-monotonic size dependence [21], with an increase down to 20 nm, followed by a steady decrease at lower sizes.

Before considering QSEs as one of the factors contributing to the observed behavior in our nanostructured films, it is important to establish that the electronic wavefunction is substantially confined within the grains such that the system as a whole behaves like a disordered network of weakly coupled Josephson junctions with a well defined  $T_C$ . In such



**Figure 3.** (a) Particle size ( $D$ ) dependence of the superconducting transition temperature ( $T_C$ ) of Pb obtained from electrical transport (circles) and magnetic susceptibility (triangles). The size dependence of  $T_C$  for Nb (diamonds) (from [13]) is shown for comparison (squares). (b) Variation of the upper critical field ( $H_{C2}$ ) with particle size obtained from magnetoresistance data.



**Figure 4.** Current versus voltage ( $I-V$ ) characteristics of nanostructured Pb films with different average particle sizes for increasing and decreasing currents. The pronounced hysteresis in the  $I-V$  characteristics indicates the weakly coupled nature of the grain boundaries. The particle size and the temperature at which the measurement was carried out are shown in the legend.

a network one expects to observe a large hysteresis in the  $I-V$  characteristics [22, 13] associated with the critical current and the retrapping current of the Josephson junctions in the network. Such a hysteresis has been previously shown to persist even when there is a large distribution in the junction parameters. Figure 4 shows the current versus voltage ( $I-V$ ) measurements carried out on films with different particle sizes. All the nanostructured films exhibit pronounced hysteresis in the  $I-V$  characteristics, implying that the superconducting grains are weakly coupled. Some of the  $I-V$  curves show a knee in the retrapping current, which indicates that there is a distribution in the junction parameters [22].

The evolution of the superconducting gap ( $\Delta$ ) with both size and temperature was obtained from four-probe  $I-V$  measurements down to 2.2 K, in planar tunnel junctions of  $\text{Al}/\text{Al}_2\text{O}_3/\text{nano-Pb}$ . Figure 5(a) shows the differential conductance,  $G(V) = dI/dV$ , of the films with  $D_{\text{XRD}} = 64$ ,

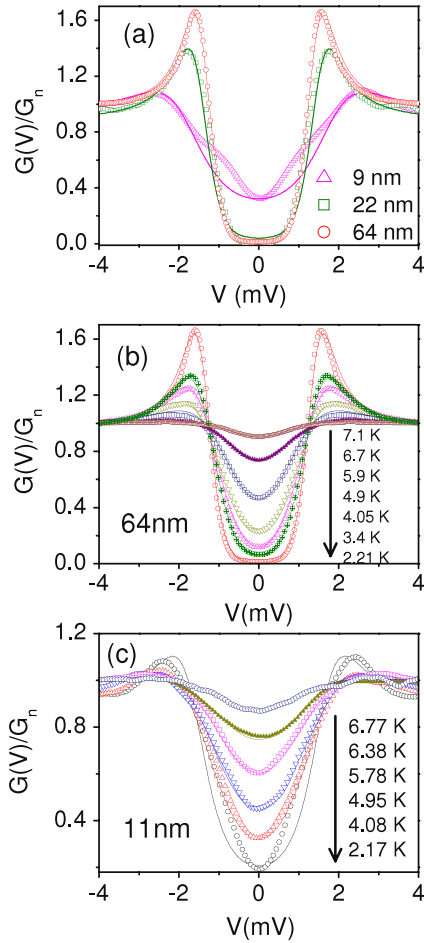


**Figure 5.** (a) Tunneling spectra of the three nanostructured superconducting films measured at 2.2 K with  $D_{\text{XRD}} = 64$  nm, 22 nm and 9 nm, respectively. Tunneling spectra (normalized differential conductance versus applied voltage) recorded at different temperatures for the nanostructured Pb films with (b)  $D_{\text{XRD}} = 64$  nm and (c)  $D_{\text{XRD}} = 11$  nm. For (a)–(c), the symbols denote the experimental points and the solid lines are the theoretical fits.

22 and 9 nm measured at 2.2 K. The data were normalized with respect to the conductance values ( $G_n$ ) between 3 and 4 mV to avoid the phonon contribution that occurs at higher bias. A visual inspection of the three graphs suggests that the superconducting energy gap increases with decreasing particle size though the spectra also get broader with decreasing size. Figures 5(b) and (c) show plots of the differential conductance,  $G(V) = dI/dV$ , versus voltage for the samples with  $D_{\text{XRD}} = 64$  nm and 11 nm, respectively, measured at different temperatures. The tunneling spectra ( $G$  versus  $V$ ) were fitted to a theoretical model for tunneling between a superconductor and a normal metal using a broadened density of states of the form [23]  $N(E, \Gamma) = \text{Re}\left(\frac{E+i\Gamma}{\sqrt{(E+i\Gamma)^2 - \Delta^2}}\right)$ . The broadening parameter,  $\Gamma = \frac{\hbar}{\tau}$ , reflects the finite lifetime ( $\tau$ ) of the superconducting quasiparticle. Thus, there are two fitting parameters,  $\Delta$  and  $\Gamma$ , for each temperature. The gap, obtained by fitting the tunneling spectra, increases from its bulk value [24],  $\Delta(0) \approx 1.38$  meV for the film with  $D_{\text{XRD}} = 64$  nm to  $\Delta(0) \approx 1.88$  meV for  $D_{\text{XRD}} = 9$  nm

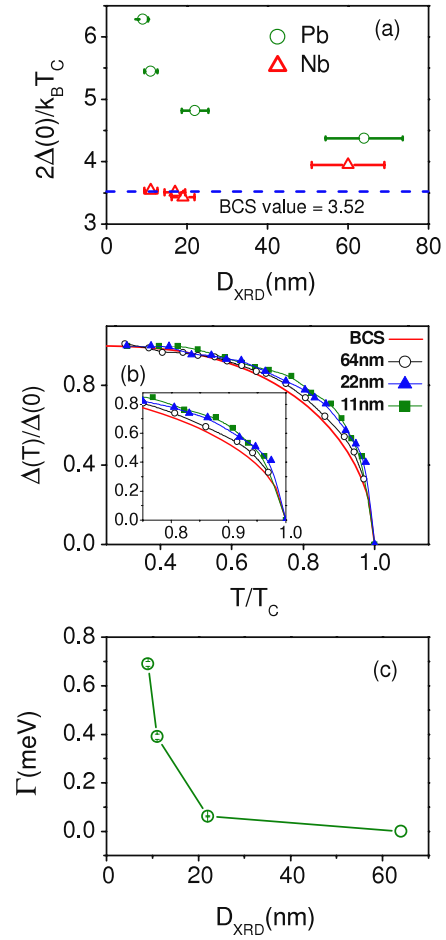


**Figure 6.** (a) Size dependence of the coupling strength,  $2\Delta(0)/k_B T_C$ , for Pb and Nb [13]. (b) Variation of the normalized superconducting energy gap with reduced temperature for Pb films with  $D_{\text{XRD}} = 64$ , 22 and 11 nm. The solid line is the temperature variation of the gap obtained from the weak coupling BCS equation. The inset shows an expanded portion of the same data showing more clearly the increasing deviation from weak coupling behavior close to  $T_C$ . (c) Variation of the broadening parameter  $\Gamma$  with particle size for nanostructured Pb films.

( $T_C = 6.9$  K). Correspondingly,  $2\Delta(0)/k_B T_C$  increases from 4.37 for the 64 nm sample to 6.28 at 9 nm (figure 6(a)). In contrast, in nanostructured Nb,  $2\Delta(0)/k_B T_C$  remains close to the BCS value in the same size range [13]. The size-dependent increase in the coupling strength can be independently inferred from the temperature variation of the superconducting gap (figure 6(b)). For a strong coupling superconductor,  $\Delta$  at finite temperature is larger than the value expected from BCS theory. This deviation from BCS theory progressively increases with increase in electron–phonon coupling strength. Since bulk Pb is a strong coupling superconductor, the normalized value of  $\Delta$  deviates slightly from the weak coupling BCS curve. A small but progressive increase of this deviation towards the strong coupling limit is observed as the particle size is reduced. Thus, Pb becomes a progressively stronger coupling superconductor in the nanocrystalline state. Along with the increase in  $\Delta$ , we also observe a systematic increase in  $\Gamma$  with a reduction in the particle size (figure 6(c)) at the lowest



temperature. (The temperature dependence also reveals that  $\Gamma$  diverges close to  $T_C$ .) This possibly reflects a decrease in the quasiparticle lifetime, expected in superconducting nanoparticles due to size induced disorder. However, since a distribution of superconducting energy gaps arising from the distribution of particle size also contributes to some extent to the broadening of the tunneling spectrum [25]<sup>6</sup>, we cannot conclusively establish the magnitude of this effect from large area tunnel junction measurements [26]<sup>7</sup>.

We can also explain the monotonic increase in  $H_{C2}$  down to 7 nm within the above scenario. The upper critical field is given by  $H_{C2} = \frac{\phi_0}{2\pi\xi_0 l_{\text{eff}}}$ , where  $\phi_0$  is the flux quantum,  $\xi_0 [\propto 1/T_C N(0)]$  is the Pippard coherence length and  $l_{\text{eff}}$  is the electronic mean free path. The observed increase in  $H_{C2}$  with size reduction indicates that the decrease in the effective mean free path due to a higher fraction of grain boundaries in the nanostructured system overrides the effect of the decrease in the product [ $T_C N(0)$ ] that would arise from the QSE, at least in the intermediate size range.

The increase in the electron–phonon coupling strength with decreasing size, inferred from the temperature dependence of the superconducting gap, implies that phonon softening plays an important role in influencing  $T_C$  in this strong coupling superconductor. The weak coupling BCS equations for  $T_C$  are thus no longer valid in the nanostructured system. In the strong coupling limit,  $T_C$  is given by McMillan’s equation [15],  $T_C = \frac{\Theta_D}{1.45} \exp\left[\frac{-1.04(1+\lambda)}{\lambda - \mu^*(1+0.62\lambda)}\right]$ , where  $\Theta_D$  is the Debye temperature and  $\mu^*$  is the effective electron–electron repulsion term. McMillan also showed that  $\lambda$  is approximately proportional to the inverse of the average squared phonon frequency:  $\langle\omega^2\rangle_M = \langle\omega\rangle/(1/\omega)$ . Thus, a reduction in  $\langle\omega^2\rangle_M$  should lead to an increase in  $\lambda$ . It is clear from McMillan’s equation that a higher coupling strength (due to size reduction) should produce higher  $T_C$ . In fact, the enhanced  $T_C$  observed in nanostructured, weak coupling superconductors such as Al, Sn, Ga and In is ascribed to phonon softening due to surface effects. Why do we not observe a similar increase in  $T_C$  in the strong coupling superconductor Pb? A plausible explanation for the observed size independence of  $T_C$  is the cancelation of the opposing influences of phonon softening and QSE [27]<sup>8</sup>. The quantization of the electronic wavevector arising from the discretization of the energy levels at small sizes cannot be neglected since it leads to the Anderson criterion that correctly predicts the observed destabilization of superconductivity at 6 nm in Pb. Also, from our measurements of  $T_C$  and  $\Delta$  in nanostructured Nb, we know

that the QSE plays a dominant role [13] in influencing  $T_C$  by decreasing the density of states at the Fermi level in small particles. We therefore believe that phonon softening effects (that tend to increase  $T_C$ ) are almost exactly offset by the QSE (that tend to decrease  $T_C$ ) in Pb down to 14 nm, resulting in a size invariant  $T_C$ . Between 14 and 7 nm, the QSE dominates and produces a 13% decrease in  $T_C$ . Below 7 nm, Pb is no longer superconducting.

We can also try to understand why the effect of phonon softening is not observed in nanostructured Nb films. We recall that in the nanostructured thin films used in our study, the superconducting grain is actually capped by an insulating layer of metal oxide. It has been shown by Tamura [28] that the contact of a nanoparticle with a harder capping layer can significantly increase the energy of the surface phonon mode, thereby reducing the effect of phonon softening. Therefore, whether we observe the effect of phonon softening depends on the hardness of the oxide layer capping it. Since the oxides of Nb have melting points which are roughly double those for the oxides of Pb [29], we may expect that the capping layer on Nb nanoparticles is significantly harder. This is the possible reason why we do not see the effect of phonon softening in nanostructured Nb films.

It is also worth noting that contrary to the strong coupling superconductor Pb, in weak coupling superconductors surface phonon softening leads to an increase in  $T_C$  with reduction in particle size and is not offset by QSEs. This difference could arise from the fact that in bulk strong coupling superconductors the phonons are present at lower frequencies compared to their weak coupling counterparts. Any change in the phonon frequencies due to size effects will therefore not lead to an appreciable effect of phonon softening in strong coupling systems. Hence, the increase in the electron–phonon coupling strength due to surface phonon softening will be lower compared to weak coupling superconductors, and can be offset by QSEs.

Finally, we would like to note that while the competition between surface phonon softening seems at present the most likely explanation for the relative robustness of  $T_C$  and the large increase in  $2\Delta/k_B T_C$  with decreasing particle size, there is at least one other possible scenario which could also explain these observations. In a recent paper [30], Feigel’man *et al* have suggested that in a strongly disordered granular superconductor the single particle excitation gap can be much larger than the superconducting energy gap, giving rise to anomalously large values of  $2\Delta/k_B T_C$ . However, at present, there is not sufficient information on this scenario to make a detailed comparison with experiments.

In summary, we have reported a detailed investigation of the evolution of superconductivity with particle size in nanostructured films of Pb. Measurements of the superconducting energy gap and the critical field in nanostructured Pb indicate a deviation from the weak coupling BCS behavior. This suggests an increase in the electron–phonon coupling strength with a reduction in the particle size in nano-Pb. The expected increase in  $T_C$  due to this effect is, however, not observed, being almost exactly offset by the QSE. Below 7 nm, QSEs dominate and superconductivity

<sup>6</sup> It has been shown in the context of anisotropic superconductors that the conductance spectrum arising from a distribution of superconducting energy gaps can be fitted by incorporating the broadening parameter  $\Gamma$ .

<sup>7</sup> Scanning tunneling spectroscopy measurements on isolated Pb islands also reveal a large increase in the broadening parameter  $\Gamma$ .

<sup>8</sup> We point out in this context that Ziembra and Bergman [27] had earlier reported an increase in  $2\Delta(0)/k_B T_C$  in disordered thin films of Pb deposited at low temperatures. They had qualitatively explained their results on the basis of an increase in the electron–electron attractive interaction in the presence of disorder. However, their arguments were based on the enhancement of electron–electron interaction through scattering by crystal imperfections, where the quantization of the electronic wavevector arising from the finite size of the superconducting grains was not taken into account. As our films consist of weakly coupled superconducting grains, we believe that the effects of surface phonon softening and discretization of the electronic wavevector should play a more dominant role.

is destroyed, consistent with the Anderson criterion. Our studies provide a natural explanation for the robustness of the superconducting transition temperature in nanosized Pb particles almost down to the theoretical limit at which superconductivity is destabilized.

### Acknowledgments

We thank J John, N Kulkarni and V Bagwe for technical assistance and Dr A Shanenko for useful discussions.

### References

- [1] Matsuo S, Sugiura H and Noguchi S 1974 *J. Low Temp. Phys.* **15** 481
- [2] Anderson P W 1959 *J. Phys. Chem. Solids* **11** 26
- [3] Oshima K, Kuroishi T and Fujita T 1976 *J. Phys. Soc. Japan* **41** 1234
- [4] Abeles B, Cohen R W and Cullen G W 1966 *Phys. Rev. Lett.* **17** 632
- [5] Rao N A H K, Garland J C and Tanner D B 1984 *Phys. Rev. B* **29** 1214  
Tsuboi T and Suzuki T 1977 *J. Phys. Soc. Japan* **42** 437
- [6] Reich S, Leitus G, Popovitz-Biro R and Schechter M 2003 *Phys. Rev. Lett.* **91** 147001
- [7] Li W H, Yang C C, Tsao F C and Lee K C 2003 *Phys. Rev. B* **68** 184507
- [8] Jaeger H M, Haviland D B, Orr B G and Goldman A M 1989 *Phys. Rev. B* **40** 182 and references therein
- [9] Hihara T, Yamada Y, Katoh M, Peng D L and Sumiyama K 2003 *J. Appl. Phys.* **94** 7594
- [10] Barber R P Jr, Merchant L M, La Porta A and Dynes R C 1994 *Phys. Rev. B* **49** 3409  
Frydman A, Naaman O and Dynes R C 2002 *Phys. Rev. B* **66** 052509
- [11] Ralph D C, Black C T and Tinkham M 1995 *Phys. Rev. Lett.* **74** 3241
- [12] Li W-H, Yang C C, Tsao F C, Wu S Y, Huang P J, Chung M K and Yao Y D 2005 *Phys. Rev. B* **72** 214516
- [13] Bose S, Raychaudhuri P, Banerjee R, Vasa P and Ayyub P 2005 *Phys. Rev. Lett.* **95** 147003
- [14] Dickey J M and Paskin A 1968 *Phys. Rev. Lett.* **21** 1441
- [15] McMillan W L 1968 *Phys. Rev.* **167** 331
- [16] Strongin M, Thompson R S, Kammerer O F and Crow J E 1970 *Phys. Rev. B* **1** 1078
- [17] Strongin M, Kammerer O F, Crow J E, Parks R D, Douglass D H and Jensen M A 1968 *Phys. Rev. Lett.* **21** 1320
- [18] Bose S, Banerjee R, Genc A, Raychaudhuri P, Fraser H L and Ayyub P 2006 *J. Phys.: Condens. Matter* **18** 4553
- [19] Giaever I 1960 *Phys. Rev. Lett.* **5** 147  
Giaever I 1960 *Phys. Rev. Lett.* **5** 464
- [20] Kittel C 1976 *Introduction to Solid State Physics* 5th edn (New York: Wiley)
- [21] Bose S, Raychaudhuri P, Banerjee R and Ayyub P 2006 *Phys. Rev. B* **74** 224502
- [22] Gupta K D, Soman S S, Sambandamurthy G and Chandrasekhar N 2002 *Phys. Rev. B* **66** 144512
- [23] Dynes R C, Garno J P, Hertel G B and Orlando T P 1984 *Phys. Rev. Lett.* **53** 2437
- [24] Giaever I and Megerle K 1961 *Phys. Rev.* **122** 1101  
Townsend P and Sutton J 1962 *Phys. Rev.* **128** 591
- [25] Raychaudhuri P, Jaiswal-Nagar D, Goutam S, Ramakrishnan S and Takeya H 2004 *Phys. Rev. Lett.* **93** 156802
- [26] Nishio T, Ono M, Eguchi T, Sakata H and Hasegawa Y 2006 *Appl. Phys. Lett.* **88** 113115
- [27] Ziemba G and Bergmann G 1970 *Z. Phys.* **237** 410
- [28] Tamura A 1993 *Z. Phys. D* **26** (suppl.) 240
- [29] WebElements™ periodic table <http://www.webelements.com>
- [30] Feigel'man M V, Ioffe L B, Kravtsov V E and Yuzbashyan E A 2007 *Phys. Rev. Lett.* **98** 027001